Transcranial Ultrasound Imaging with Estimating the Geometry, Position and Wave-Speed of Temporal Bone

Mozaffarzadeh, Moein; Verweij, Martin D.; Daeichin, Verya; de Jong, Nico; Renaud, Guillaume

DOI
10.1109/IUS52206.2021.9593826

Publication date
2021

Document Version
Final published version

Published in
2021 IEEE International Ultrasonics Symposium (IUS)

Transcranial Ultrasound Imaging with Estimating the Geometry, Position and Wave-Speed of Temporal Bone

Moein Mozaffarzadeh*
Department of Imaging Physics
Technical University of Delft
Delft, The Netherlands
m.mozaffarzadeh@tudelft.nl

Martin D. Verweij
Department of Imaging Physics
Technical University of Delft
Delft, The Netherlands
M.D.Verweij@tudelft.nl

Verya Daeichin
Department of Imaging Physics
Technical University of Delft
Delft, The Netherlands
V.Daeichin@tudelft.nl

Nico de Jong
Department of Imaging Physics
Technical University of Delft
Delft, The Netherlands
Nicolaas.deJong@tudelft.nl

Guillaume Renaud
Department of Imaging Physics
Technical University of Delft
Delft, The Netherlands
G.G.J.Renaud@tudelft.nl

***Abstract*—Transcranial ultrasound imaging is a suitable technology for diagnosis of strokes as it is safe, portable, relatively inexpensive and available in emergency medicine services, however it currently offers poor image quality due to the phase aberration caused by the human skull. In this work, we evaluate an approach for two-dimensional transcranial ultrasound imaging through the temporal window of a sagittally-cut human skull using the commercial P4-1 phased-array probe, where the position and true geometry of the bone layer is estimated for accurate phase aberration correction. The medium is described with four layers (probe lens, soft tissue, skull, soft tissue). A synthetic aperture imaging scheme is used as the transmission of spherical wave-fronts facilitates the modeling of refraction. First, the bidirectional headwave method estimates the compressional wave-speed in the temporal bone. Next, a fast marching method calculates the travel times between individual array elements and image pixels to be used with delay-and-sum reconstruction algorithm. Sound speed maps are generated with adaptive beamforming including the successive segmentation of the near and far surfaces of the cortical bone layer. The proposed method reconstructs the scatterers with an average lateral and axial localization error of about 1.25 mm and 0.37 mm, compared to the ground truth, respectively. In average, it improves the contrast ratio and lateral resolution by 7 dB and 36%, compared to the conventional method, respectively.**

Keywords— Transcranial ultrasound imaging; Adaptive beamforming; Phase aberration correction; Head wave; Temporal bone

I. Introduction

Despite all the advantages transcranial ultrasound imaging (TUI) provides in clinical applications (such as stroke diagnosis [1, 2] and detection of microemboli [3, 4]) and imaging technologies (such as ultrasound localization microscopy [5-7] and functional ultrasound imaging [8, 9]), it is still hindered due to strong aberration and scattering [10] and multiple reflections caused by the skull [11, 12].

Usually, the temporal window of human skull is used for TUI as 1) it enables imaging of the arteries of the circle of Willis and 2) the squamous part of the temporal bone often consists of a single layer of cortical bone with a thickness, mass density and one-way attenuation at normal incidence of 1.5 to 4.4 mm [13-16] and 1700 to 2000 kg/m3 [16] and 13 to 22 dB/cm/MHz [17], respectively. Whereas, the one-way attenuation through the other parts of skull (can be as thick as 1 cm) can exceed 25 dB/cm/MHz for a diploe thickness of 6 mm [10].

Looking into the past decade, different methods have been developed to compensate the phase aberration caused by the skull [18]. There are two main approaches: 1) the phase screen model in which the skull is modeled as an infinitesimally thin aberrating layer at the surface of the transducer [11, 19], and 2) using information about the true geometry and compressional wave-speed of the skull to correct refraction during image reconstruction. The former limits the improvements to certain regions called isoplanatic patches [20]. The latter is more practical, especially in emergency medicine services, if the same ultrasound probe is used to obtain the geometry and compressional wave-speed of the skull [21-23], but not CT or MRI scans [24-27].

In this paper, we use the physics of ultrasound wave propagation through a single-layer cortical bone for correcting phase aberration. The goal is to improve two-dimensional transcranial ultrasound B-mode images. The novelty of our approach lies in the fact that the position and true geometry of the bone layer and the compressional wave-speed in the cortical bone of the temporal window are estimated with the same probe used for ultrasound imaging. To the best of the authors' knowledge, this is the first report on the feasibility of single-sided refraction-corrected two-dimensional transcranial ultrasound imaging through the human temporal window using a single commercial probe.

II. Materials and Methods

A. Proposed image reconstruction approach

Our image reconstruction approach consists of six steps:

1- Image reconstruction with the primary velocity model (lens, water).
2- Segmentation of the near surface of the aberrator.
3- Estimation of the wave-speed in the aberrator with the headwave method.
4- Updating the velocity model (lens, water, aberrator) + Image reconstruction.
5- Segmentation of the far surface of the aberrator.
6- Updating the velocity model (lens, water, aberrator, water) + Image reconstruction.

A synthetic aperture scheme was used for imaging as the transmission of spherical wave-fronts facilitates the

2021 IEEE International Ultrasonics Symposium (IUS) | 978-1-6654-0355-9/21/$31.00 ©2021 IEEE | DOI: 10.1109/IUS52206.2021.9593826

modeling of refraction (necessary for phase correction) and provides dynamic focusing in transmission [28], which helps with a better extraction of the velocity model.

Delay-and-sum (DAS) beamformer was used to apply dynamic focusing in reception [28, 29]. Its formula is as:

$$I(p)=\sum_{i=1}^{M}\sum_{i=1}^{N} RF(t=t_T(i,p)+t_R(j,p),i,j) \times W(P,i,j), \quad (1)$$

where, I is the output of the beamformer at pixel p, M and N are the number of transmissions and receivers, respectively, RF is the recorded data, t_T and t_R are the transmit and receive travel times, respectively, and $W(P,i,j)$ is a weight calculated for pixel p. In this paper, this weight is based on the far field directivity of the elements of the array [30, 31]. To accurately reconstruct the images, the phase aberration caused by the skull (directly affecting the arrival times used for beamforming) should be taken into account. To this end, the fast marching technique (FMT) was used. FMT solves the Eikonal equation and calculates the travel times given a velocity model [32, 33].

A technique based on Dijkstra's algorithm was used for segmentation of the surfaces [34, 35]. The segmentation algorithm seeks the shortest path that follows the interface with the highest intensity in the ultrasound image, by maximizing a merit; here the sum of the pixel intensities along the path.

The bidirectional headwave method (based on the first arriving signal along a flat interface) was used to estimate the compressional wave speed within the plane of the temporal bone [36]. As an isotopic temporal bone is assumed in this study, the wave-speed estimated by the bidirectional headwave method is equal to that in the direction normal to the surface of the skull [37].

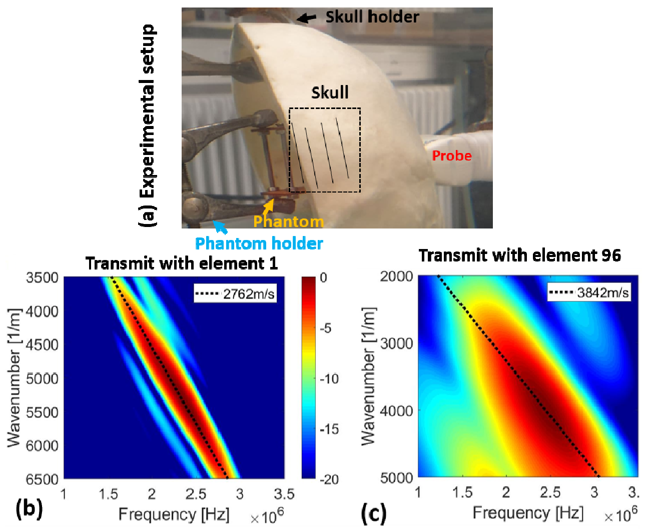

Fig. 1. (a) The experimental setup. The lines inside the dashed box schematically show the wires that are placed perpendicular to the imaging plane. (b,c) Estimation of the wave-speed in the temporal bone with the measurement of the headwave velocity. The experimental f-k domain data when element 1 and 96 transmit a spherical wave, respectively.

B. *Experimental study*

We conducted an experiment with a sagittally-cut human skull to validate the proposed image reconstruction approach (see Fig. 1(a)). The human skull (Skulls Unlimited International Inc.) was carefully prepared with the use of dermestid beetles. Before experiments, the skull was degassed at 80 mBar for 48 hours.

A phantom including multiple wires (50 µm diameter)

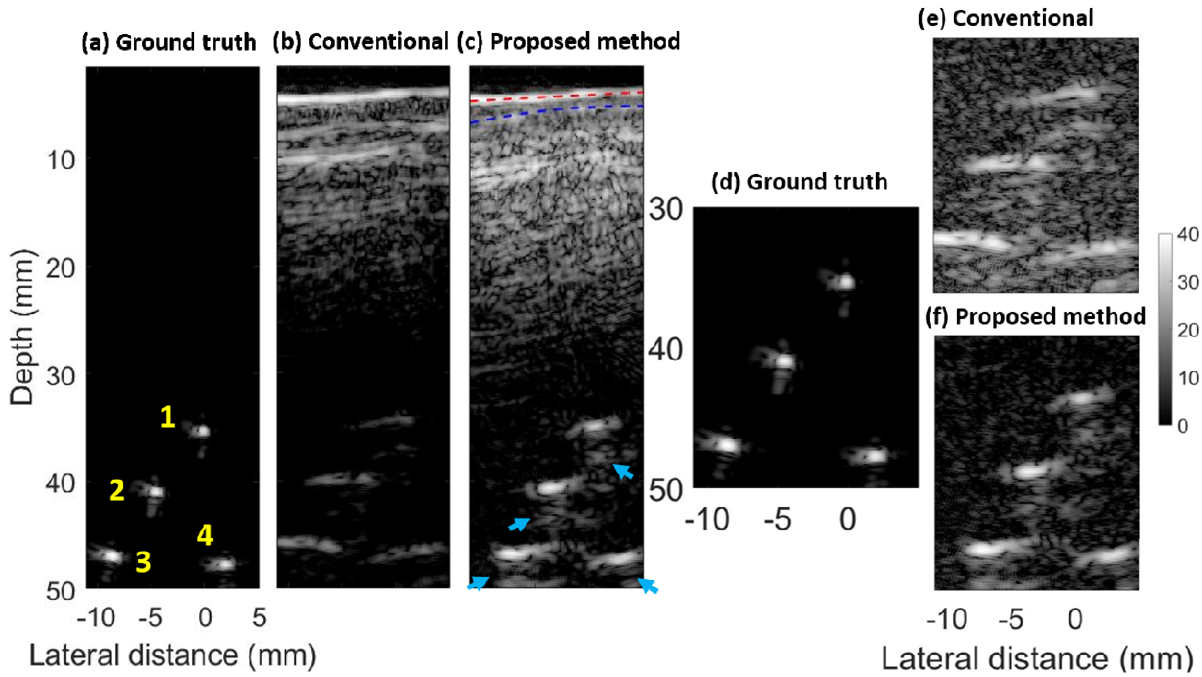

Fig. 2. The reconstructed images (a) without and (b, c) with the skull in front of the probe. (d-f) are the zoomed versions of (a-c) respectively; these figures are normalized and log compressed to the local maximum. The red and blue dashed lines in (c) show the near and far (relative to the probe) surfaces of the skull, respectively. The blue arrows in (c) show the multiple reflections of scatterers.

was used. The imaging plane of the 1D probe was perpendicular to the wires. Therefore, the wires are expected to mimic point scatterers considering their diameter (about one-tenth of the wavelength at the central frequency). To have a ground truth measurement, the probe was moved against the phantom with a XYZ system, the skull was carefully removed from the setup, and finally the probe was moved back to its first place; the rest of the components were fixed. All the experiments were conducted with a P4-1 probe (ATL/Philips, 2.5 MHz, 96 elements, pitch = 0.295 mm) connected to a Verasonics Vantage 256 system.

III. RESULTS AND AND DISCUSSION

A. Experimental results

A compressional wave-speed of 3500 m/s (Fig. 1(b, c) and considering the formula of the bidirectional head-wave technique [36]) and a mean thickness of 1.3 mm (Fig. 2(c)) were measured in the temporal cortical bone; the wave-speed estimation was in agreement with [38]. The red and blue dashed lines in Fig. 2(c) show the near and far (relative to the probe) surfaces of the skull, respectively. The blue arrows in Fig. 2(c) show the multiple reflections of scatterers. Compared to the ground truth image without the skull, Fig. 2(b, e) show that the skull creates substantial clutter due to multiple scattering and suboptimal image reconstruction of the wires. The proposed method enhances the visibility of the wires (Fig. 2(c, f)) because wave physics (i.e., refraction) in the layered medium is accurately described, and hence the travel times are accurately calculated. The level of background noise is higher in Fig. 2(e), compared to Fig. 2(f), due to the distribution of energy to different pixels, which is mainly caused by the phase aberration induced by the skull. The proposed method reconstructs the scatterers with an average lateral and axial localization error of about 1.25 mm and 0.37 mm, compared to the ground truth, respectively. For the conventional method, which reconstructs an image assuming a uniform medium made of water only, these quantities are 1.5 mm, 1.2 mm, respectively. In average, it improves the contrast ratio and resolution by 7 dB and 36%, compared to the conventional method, respectively.

B. Limitations and future works

While the temporal bone was considered isotropic, the compressional wave-speed in the plane of the bone layer (estimated with the head-wave technique in our study) is 13% higher than that in the direction normal to the plane of the bone layer as reported in [38]. The autofocus method can be used to estimate the compressional wave-speed in the direction normal to the plane of the bone layer [29], and then with multiple measurements in different planes of the bone layer, an accurate velocity model could be estimated.

The near surface of the temporal window was assumed flat when estimating the wave-speed in bone with the headwave method. While this is a fair simplification considering the small footprint of the P4-1 probe and the local geometry of human skull, development of techniques to compensate for the bone curvature (in the lateral direction) and even bone irregularities could be of interest for a more accurate compressional wave-speed estimation.

The temporal bone was described as a homogeneous layer of cortical bone. Further development with a three-layer bone model (cortical-cancellous-cortical) could improve the image quality and even lower the temporal window failure rate [39].

Finally, the elevation effect of the 1D array was ignored. With a 2D matrix array transducer, we could take into account the three-dimensional shape of the temporal bone during image reconstruction.

IV. CONCLUSION

We introduced a technique, for the first time to the best our knowledge, to extract the true geometry of the human skull for correcting the phase aberration caused by the temporal bone in single-sided two-dimensional transcranial ultrasound imaging using a single commercial probe. The proposed approach led to an average lateral and axial localization error (compared to the ground truth) of 1.25 mm and 0.37 mm in an experiment consisting of imaging a wire phantom placed behind a sagittally-cut human skull, respectively. This substantially improved the image quality; contrast ratio and lateral resolution are improved by 7 dB and 36%, respectively, compared to conventional image reconstruction.

REFERENCES

[1] T. Hölscher *et al.*, "Transcranial ultrasound from diagnosis to early stroke treatment," *Cerebrovascular diseases,* vol. 26, no. 6, pp. 659-663, 2008.

[2] F. Schlachetzki *et al.*, "Transcranial ultrasound from diagnosis to early stroke treatment–Part 2: Prehospital neurosonography in patients with acute stroke–The Regensburg Stroke Mobile Project," *Cerebrovascular diseases,* vol. 33, no. 3, pp. 262-271, 2012.

[3] T. Padayachee, S. Parsons, R. Theobold, J. Linley, R. Gosling, and P. Deverall, "The detection of microemboli in the middle cerebral artery during cardiopulmonary bypass: a transcranial Doppler ultrasound investigation using membrane and bubble oxygenators," *The Annals of thoracic surgery,* vol. 44, no. 3, pp. 298-302, 1987.

[4] D. C. Tong and G. W. Albers, "Transcranial Doppler–detected microemboli in patients with acute stroke," *Stroke,* vol. 26, no. 9, pp. 1588-1592, 1995.

[5] D. E. Soulioti, D. Espíndola, P. A. Dayton, and G. F. Pinton, "Super-resolution imaging through the human skull," *IEEE transactions on ultrasonics, ferroelectrics, frequency control,* vol. 67, no. 1, pp. 25-36, 2019.

[6] C. Errico *et al.*, "Ultrafast ultrasound localization microscopy for deep super-resolution vascular imaging," *Nature methods,* vol. 527, no. 7579, pp. 499-502, 2015.

[7] C. Demené *et al.*, "Transcranial ultrafast ultrasound localization microscopy of brain vasculature in patients," *Nature Biomedical Engineering,* vol. 5, no. 3, pp. 219-228, 2021.

[8] E. Tiran *et al.*, "Transcranial functional ultrasound imaging in freely moving awake mice and anesthetized young rats without contrast agent," *Ultrasound in medicine & biology,* vol. 43, no. 8, pp. 1679-1689, 2017.

[9] J. Baranger *et al.*, "Bedside functional monitoring of the dynamic brain connectivity in human neonates," *Nature communications,* vol. 12, no. 1, pp. 1-10, 2021.

[10] F. J. Fry and J. E. Barger, "Acoustical properties of the human skull," *The Journal of the Acoustical Society of America,* vol. 63, no. 5, pp. 1576-1590, 1978.

[11] F. Vignon, J. Aubry, M. Tanter, A. Margoum, and M. Fink, "Adaptive focusing for transcranial ultrasound imaging using dual arrays," *The Journal of the Acoustical Society of America,* vol. 120, no. 5, pp. 2737-2745, 2006.

[12] G. Pinton, J. F. Aubry, E. Bossy, M. Muller, M. Pernot, and M. Tanter, "Attenuation, scattering, and absorption of ultrasound in the skull bone," *Medical physics,* vol. 39, no. 1, pp. 299-307, 2012.

[13] R. T. Brisson *et al.*, "Association between tomographic characteristics of the temporal bone and transtemporal window quality on transcranial color Doppler ultrasound in patients with

stroke or transient ischemic attack," *Ultrasound in Medicine & Biology,* vol. 47, no. 3, pp. 511-516, 2021.

[14] J. H. Kwon, J. S. Kim, D. W. Kang, K. S. Bae, and S. U. Kwon, "The thickness and texture of temporal bone in brain CT predict acoustic window failure of transcranial Doppler," *Journal of Neuroimaging,* vol. 16, no. 4, pp. 347-352, 2006.

[15] C.-H. Lee, S.-H. Jeon, S.-J. Wang, B.-S. Shin, and H. G. Kang, "Factors associated with temporal window failure in transcranial Doppler sonography," *Neurological sciences: official journal of the Italian Neurological Society and of the Italian Society of Clinical Neurophysiology,* 2020.

[16] J. Peterson and P. C. Dechow, "Material properties of the human cranial vault and zygoma," *The Anatomical Record Part A: Discoveries in Molecular, Cellular, and Evolutionary Biology: An Official Publication of the American Association of Anatomists,* vol. 274, no. 1, pp. 785-797, 2003.

[17] A. Y. Ammi *et al.*, "Characterization of ultrasound propagation through ex-vivo human temporal bone," *Ultrasound in medicine & biology,* vol. 34, no. 10, pp. 1578-1589, 2008.

[18] A. Kyriakou, E. Neufeld, B. Werner, M. M. Paulides, G. Szekely, and N. Kuster, "A review of numerical and experimental compensation techniques for skull-induced phase aberrations in transcranial focused ultrasound," *International journal of hyperthermia,* vol. 30, no. 1, pp. 36-46, 2014.

[19] J. J. Dahl, M. S. Soo, and G. E. Trahey, "Spatial and temporal aberrator stability for real-time adaptive imaging," *IEEE transactions on ultrasonics, ferroelectrics, and frequency control,* vol. 52, no. 9, pp. 1504-1517, 2005.

[20] B. D. Lindsey and S. W. Smith, "Pitch-catch phase aberration correction of multiple isoplanatic patches for 3-D transcranial ultrasound imaging," *IEEE transactions on ultrasonics, ferroelectrics, and frequency control,* vol. 60, no. 3, pp. 463-480, 2013.

[21] T. Wang and Y. Jing, "Transcranial ultrasound imaging with speed of sound-based phase correction: a numerical study," *Physics in Medicine & Biology,* vol. 58, no. 19, p. 6663, 2013.

[22] X. Lin, M. Sun, Y. Liu, Z. Shen, Y. Shen, and N. Feng, "Variable speed of sound compensation in the linear-array photoacoustic tomography using a multi-stencils fast marching method," *Biomedical Signal Processing and Control,* vol. 44, pp. 67-74, 2018.

[23] K. Shapoori, J. Sadler, A. Wydra, E. V. Malyarenko, A. N. Sinclair, and R. G. Maev, "An ultrasonic-adaptive beamforming method and its application for trans-skull imaging of certain types of head injuries; Part I: Transmission mode," *IEEE Transactions on Biomedical Engineering,* vol. 62, no. 5, pp. 1253-1264, 2014.

[24] C. Jiang *et al.*, "Ray Theory-Based Transcranial Phase Correction for Intracranial Imaging: A Phantom Study," *IEEE Access,* vol. 7, pp. 163013-163021, 2019.

[25] Y. Jing, F. C. Meral, and G. T. Clement, "Time-reversal transcranial ultrasound beam focusing using a k-space method," *Physics in Medicine and Biology,* vol. 57, no. 4, p. 901, 2012.

[26] G. Bouchoux *et al.*, "Experimental validation of a finite-difference model for the prediction of transcranial ultrasound fields based on CT images," *Physics in Medicine and Biology,* vol. 57, no. 23, p. 8005, 2012.

[27] C. Jiang, Y. Li, K. Xu, and D. Ta, "Full-Matrix Phase Shift Migration Method for Transcranial Ultrasonic Imaging," *IEEE Transactions on Ultrasonics, Ferroelectrics, and Frequency Control,* 2020.

[28] J. A. Jensen, S. I. Nikolov, K. L. Gammelmark, and M. H. Pedersen, "Synthetic aperture ultrasound imaging," *Ultrasonics,* vol. 44, pp. e5-e15, 2006.

[29] G. Renaud, P. Kruizinga, D. Cassereau, and P. Laugier, "In vivo ultrasound imaging of the bone cortex," *Physics in Medicine & Biology,* vol. 63, no. 12, p. 125010, 2018.

[30] H. Hasegawa and H. Kanai, "Effect of element directivity on adaptive beamforming applied to high-frame-rate ultrasound," *IEEE transactions on ultrasonics, ferroelectrics, and frequency control,* vol. 62, no. 3, pp. 511-523, 2015.

[31] M. Mozaffarzadeh *et al.*, "Receive/transmit aperture selection for 3D ultrasound imaging with a 2D matrix transducer," *Applied Sciences,* vol. 10, no. 15, p. 5300, 2020.

[32] J. A. Sethian, *Level set methods and fast marching methods: evolving interfaces in computational geometry, fluid mechanics, computer vision, and materials science*. Cambridge university press, 1999.

[33] M. S. Hassouna and A. A. Farag, "Multistencils fast marching methods: A highly accurate solution to the eikonal equation on cartesian domains," *IEEE transactions on pattern analysis and machine intelligence,* vol. 29, no. 9, pp. 1563-1574, 2007.

[34] E. W. Dijkstra, "A note on two problems in connexion with graphs," *Numerische mathematik,* vol. 1, no. 1, pp. 269-271, 1959.

[35] D. Hong, "Medical image segmentation based on accelerated Dijkstra algorithm," in *Advances in Intelligent Systems*: Springer, 2012, pp. 341-348.

[36] E. Bossy, M. Talmant, M. Defontaine, F. Patat, and P. Laugier, "Bidirectional axial transmission can improve accuracy and precision of ultrasonic velocity measurement in cortical bone: a validation on test materials," *IEEE transactions on ultrasonics, ferroelectrics, and frequency control,* vol. 51, no. 1, pp. 71-79, 2004.

[37] M. Mozaffarzadeh, C. Minonzio, N. De Jong, M. D. Verweij, S. Hemm, and V. Daeichin, "Lamb Waves and Adaptive Beamforming for Aberration Correction in Medical Ultrasound Imaging," *IEEE transactions on ultrasonics, ferroelectrics, and frequency control,* vol. 68, no. 1, pp. 84-91, 2020.

[38] J. Peterson and P. C. Dechow, "Material properties of the human cranial vault and zygoma," *The Anatomical Record Part A: Discoveries in Molecular, Cellular, Evolutionary Biology: An Official Publication of the American Association of Anatomists,* vol. 274, no. 1, pp. 785-797, 2003.

[39] Z. Kardos *et al.*, "Increased frequency of temporal acoustic window failure in rheumatoid arthritis: a manifestation of altered bone metabolism?," *Clinical rheumatology,* vol. 37, no. 5, pp. 1183-1188, 2018.